White Rose Research Online

eprints@whiterose.ac.uk
https://eprints.whiterose.ac.uk
Universities of Leeds, Sheffield and York

Deposited via The University of Sheffield.

White Rose Research Online URL for this paper:
https://eprints.whiterose.ac.uk/id/eprint/151625/

Version: Published Version

Article:
Bellinghausen, S.., Gavi, E., Jerke, L. et al. (2019) Nuclei size distribution modelling in wet granulation. Chemical Engineering Science: X, 4. 100038. ISSN: 2590-1400

https://doi.org/10.1016/j.cesx.2019.100038

Reuse
This article is distributed under the terms of the Creative Commons Attribution-NonCommercial-NoDerivs (CC BY-NC-ND) licence. This licence only allows you to download this work and share it with others as long as you credit the authors, but you can't change the article in any way or use it commercially. More information and the full terms of the licence here: https://creativecommons.org/licenses/

Takedown
If you consider content in White Rose Research Online to be in breach of UK law, please notify us by emailing eprints@whiterose.ac.uk including the URL of the record and the reason for the withdrawal request.

UNIVERSITY OF LEEDS
University of Sheffield
UNIVERSITY of York

Chemical Engineering Science: X 4 (2019) 100038

Contents lists available at ScienceDirect

Chemical Engineering Science: X

journal homepage: www.elsevier.com/locate/cesx

Nuclei size distribution modelling in wet granulation

Stefan Bellinghausen [a,*], Emmanuela Gavi [b], Laura Jerke [b], Pranay K. Ghosh [b], Agba D. Salman [a], James D. Litster [a]

[a] Department of Chemical and Biological Engineering, University of Sheffield, Mappin Street, Sheffield S1 3JD, UK
[b] Small Molecule Technical Development Formulation, F. Hoffmann-La Roche AG, Grenzacherstrasse 124, 4070 Basel, Switzerland

ARTICLE INFO

Article history:
Received 30 April 2019
Received in revised form 23 August 2019
Accepted 7 September 2019

Keywords:
Wet granulation
Nucleation
Monte Carlo simulations
Poisson distribution
Dimensionless nucleation number

ABSTRACT

Nucleation is an important wet granulation rate process that sometimes has a profound effect on granule attributes and which needs to be captured in process modelling studies. However, existing models fail to predict nuclei size distribution of a range of spray conditions typically used in industry. In this paper, the dimensionless nucleation number Ψ_n is used to develop two new nuclei size distribution models, one empirical and one semi-mechanistic. The empirical model assumes a log-normal distribution (LND), and the semi-mechanistic model is based on a approach proposed by Hapgood et al. (2009), which applies the Poisson distribution (PD) function. Modelling parameters are estimated using Monte Carlo simulations (MCS) data. From the models, the nuclei size distribution can be easily determined using analytical equations, which simplifies the inclusion in a population balance modelling (PBM) framework. The results of both models are assessed using MCS data as well as experimental data from literature. The empirical LND model is able to capture the MCS results accurately, and the predictions agree reasonably well with the experimental results over a wide range of dimensionless nucleation number ($0 < \Psi_n < 3$). The predictions of the semi-mechanistic modified Poisson distribution (MPD) model do not agree qualitatively with the MCS or experimental results. A sensitivity analysis shows that the MCS modelling assumptions need to capture the spatial drop distribution in the spray accurately, while the drop size distribution can be assumed to be uniform. Overall, we recommend that the LND model with the parameter values estimated be used in PBM frameworks to determine nuclei size distribution for a wide range of experimental conditions in mixers and fluidised granulators.

© 2019 Published by Elsevier Ltd. This is an open access article under the CC BY-NC-ND license (http://creativecommons.org/licenses/by-nc-nd/4.0/).

1. Introduction

Wet granulation is a size enlargement process whereby granules are formed from a particulate feed using a liquid binder. This process is ubiquitous in any industry processing fine powders. Different equipment is available for wet granulation including fluidised bed granulators, high-shear mixers and twin-screw granulators. The granule attributes are controlled by three classes of rate processes that occur during granulation: wetting and nucleation, consolidation, layering and coalescence, and breakage and attrition. If the kinetics of these rate processes are known, then predictive models for wet granulation processes are possible.

The most promising approach to model wet granulation rate processes at the macroscopic scale is a population balance modelling (PBM) framework. The population balance equation for wet granulation can be written as (Ramkrishna and Mahoney, 2002):

$$\frac{\partial Vn(\bar{x},t)}{\partial t} + \frac{\partial}{\partial \bar{x}}\left[Vn(\bar{x},t)\left(\dot{G}_{lay} + \dot{G}_{cons}\right)\right] = \dot{V}_{in}n_{in}(\bar{x}) - \dot{V}_{out}n_{out}(\bar{x}) + V\left[\dot{b}_{nuc}(\bar{x}) + \dot{b}_{coal}(\bar{x}) + \dot{b}_{br}(\bar{x}) - \dot{d}_{coal}(\bar{x}) - \dot{d}_{br}(\bar{x})\right], \quad (1)$$

where V is the control volume, n is the volume-specific number density of particles, $\bar{x}$ is the set of granule properties of interest, t is time, $\dot{V}_{in}$ and $\dot{V}_{out}$ are the entering and leaving volumetric flowrates, $\dot{G}_{lay}$ and $\dot{G}_{cons}$ are the rate of change due to layering and consolidation, respectively, $\dot{b}_{nuc}, \dot{b}_{coal}$ and $\dot{b}_{br}$ are the birth rates due to nucleation, coalescence and breakage, and $\dot{d}_{coal}$ and $\dot{d}_{br}$ are the death rates due to coalescence and breakage. PBM has been widely applied to wet granulation (Ramachandran et al., 2009; Kastner et al., 2013; Biggs et al., 2003; Darelius et al., 2006; Lee et al.,

Abbreviation: LND, Log-normal distribution; MCS, Monte Carlo simulations; MPD, Modified Poisson distribution; PBM, Population balance modelling; PD, Poisson distribution.

* Corresponding author.
E-mail address: sbellinghausen1@sheffield.ac.uk (S. Bellinghausen).

https://doi.org/10.1016/j.cesx.2019.100038
2590-1400/© 2019 Published by Elsevier Ltd.
This is an open access article under the CC BY-NC-ND license (http://creativecommons.org/licenses/by-nc-nd/4.0/).

Nomenclature

List of Indices

1	single drop
br	breakage
coal	coalescence
cons	consolidation
d	diameter
d	drop
i, j, k	indices
lay	layering
n	nucleation
n	nuclei
nuc	nucleation
x	coordinate

List of Symbols

$\dot{A}$	area flux of the powder bed surface area through the spray zone [$\frac{m^2}{s}$]
a	cross-sectional area [m^2]
$\dot{b}$	volume-specific birth rate [$m^{-3}\ s^{-1}$]
B	subregion area [m^2]
b	fitting parameter [–]
c	fitting parameter [–]
$\dot{d}$	volume-specific death rate [$m^{-3}\ s^{-1}$]
d	diameter [m]
d'	dimensionless diameter [–]
f'_m	dimensionless mass frequency [–]
f_m	mass frequency [m^{-1}]
G	rate of change [$m^{-3}\ s^{-1}$]
i, j, k	indices [–]
K	nucleation size ratio [–]
k	nuclei exclusion area ratio [–]
$m_{1...3}$	fitting parameters [–]
N	distribution function [–]
n	number of drops [–]
n	volume-specific number density [m^{-3}]
P	probability of coalescence [–]
$s_{1...3}$	fitting parameters [–]
t	time [s]
$\dot{V}$	volumetric flowrate [$\frac{m^3}{s}$]
V	volume [m^3]
x	coordinate [m]
x	set of fitting parameters [–]
x	set of granule properties [–]
y	coordinate (direction of powder flow) [m]
λ	intensity function [–]
μ	logarithmic mean [–]
Ψ_a	dimensionless spray flux [–]
Ψ_n	dimensionless nucleation number [–]
σ	logarithmic standard deviation [–]

2017; Wauters et al., 2003; Bouffard et al., 2012; Yu et al., 2017; Le et al., 2009; Oullion et al., 2009; Sanders et al., 2003; Verkoeijen et al., 2002; Chaudhury et al., 2014; Žižek et al., 2013; Pohlman and Litster, 2015; Dhanarajan and Bandyopadhyay, 2007; Barrasso et al., 2015; Kumar et al., 2016; Poon et al., 2008).

In PBM, the key step of the model development process is to represent the most important rate processes by including appropriate kernels. In order to develop a predictive model, kernels which take full account of the impact of formulation and process variables should be applied (Chaudhury et al., 2017; Kumar et al., 2013). By far the most effort in the literature has been on the development of mechanistic kernels for coalescence. By contrast, few nucleation kernels have been developed and implemented within a PBM framework.

Nucleation is one of the important rate processes in wet granulation which describes the penetration of binder drops into a powder bed and the subsequent formation of nuclei granules. If the drop size is significantly larger than the size of the powder particles, the size of the binder liquid drops is critical for determining the nuclei size. This phenomena is also called immersion or penetration nucleation and is dominant in most high-shear wet granulation and twin-screw granulation processes. Nucleation of large particles and small drops is known as distribution nucleation (Kariuki et al., 2013) and is out of the scope of this paper.

Based on experiments, Hapgood et al. (2003, 2004) identified three different nucleation regimes for immersion nucleation (Fig. 1): drop-controlled, intermediate, and mechanical dispersion regime. In the drop-controlled regime, only few drops coalesce, hence the nuclei size distribution is rather narrow. In the mechanical dispersion regime, the conditions lead to the formation of large nuclei (lumps), which need to be broken up mechanically. By evaluating two dimensionless groups, dimensionless spray flux Ψ_a and dimensionless drop penetration time τ_p, the prevailing regime can be identified. The dimensionless spray flux Ψ_a is defined as the ratio of the flux of the area wetted to the flux of the powder bed surface area as it passes through the spray zone (Eq. (2)) (Litster et al., 2001). Drop penetration is described in more detail by Hapgood et al. (2002, 2003).

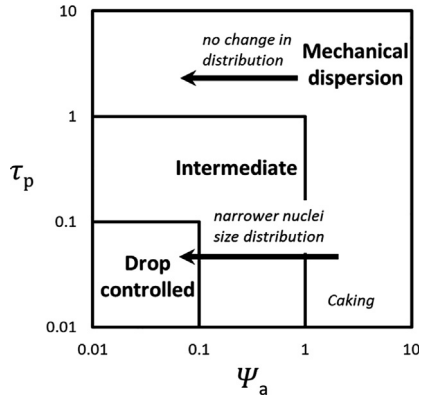

Fig. 1. Nucleation regime map (Ψ_a dimensionless spray flux, τ_p dimensionless drop penetration time) (Hapgood et al., 2003).

$$\Psi_a = \frac{3\dot{V}}{2\dot{A}d_d}, \tag{2}$$

where $\dot{V}$ is the volumetric spray rate, $\dot{A}$ is the flux of the powder bed surface area through the spray zone, and d_d is the drop diameter. A correlation between the dimensionless spray flux and the nuclei size distribution has been observed experimentally (Tardos et al., 1997; Hapgood et al., 2004; Wildeboer et al., 2007; Ax et al., 2008).

Few nucleation models have been incorporated in PBM frameworks. Poon et al. (2008, 2009) proposed a model to capture the kinetics of drop penetration. Two approaches to kinetically model nuclei formation by immersion have been developed by Hounslow et al. (2009) and compared to experimental findings by Pitt et al. (2018). A framework to determine the nuclei size based on drop size has been proposed by Barrasso and Ramachandran (2016). A frame-

work to include a spray/nucleation zone in compartmental PBM by determining its volume mechanistically has been proposed by Yu et al. (2016). None of these models predict the impact of the dimensionless spray flux Ψ_a on the nuclei size distribution due to drop coalescence and therefore are not applicable outside the drop-controlled regime. However, operating in the drop-controlled regime is challenging and sometimes impracticable, due to the very low spray rate required. A nucleation kernel that includes drop coalescence and predicts the effect of the dimensionless spray flux Ψ_a is needed to develop a PBM framework for wet granulation.

Approaches to predict the nuclei size distribution for formulations with short drop penetration times can be found in the literature. Hapgood et al. (2004) applied Monte Carlo simulations (MCS) to determine the nuclei size distribution assuming a uniform distribution of drops, spatial randomness, and a uniform drop diameter. Apart from the drop diameter, the dimensionless spray flux Ψ_a is the only input parameter. Wildeboer et al. (2005) extended the approach developed by Hapgood et al. (2004). They considered a log-normal distribution for the initial drop diameter. Furthermore, a truncated normal distribution of drops has been assumed over the width of the spray zone; this assumption is based on spray characteristics experiments by Wauters et al. (2002). This new approach explicitly takes nuclei coalescence into account. While a drop penetrates the powder bed, it forms a nuclei which is larger in size than the drop due to the addition of solid and gas. Nuclei coalescence can happen when two nuclei collide or overlap during their formation. Due to the increase in size, the probability of coalescence is higher under this assumption. The size increase can be quantified by the diameter ratio of the nuclei to the drop. Wildeboer et al. (2005) incorporated this nuclei-to-drop diameter ratio K_d and introduced the dimensionless nucleation number Ψ_n as a new dimensionless group for nuclei coalescence:

$$\Psi_n = K_d^2 \frac{3\dot{V}}{2\dot{A}d_d} = K_d^2 \Psi_a. \tag{3}$$

However, the MCS approach of Wildeboer et al. (2005) is unsuitable for process modelling studies due to long simulation times.

An analytical approach to predict the nuclei size distribution has been proposed by Hapgood et al. (2004). Here, the probabilistic Poisson distribution (PD) function has been applied with the dimensionless spray flux as input parameter. The model results showed good agreement with MCS data for powder bed surface area covered and fraction of nuclei formed by single drops. This approach has been extended by Hapgood et al. (2009) to determine the probability of drop coalescence based on the dimensionless spray flux. By comparing the results of the PD model to experimental data, they showed that this model is able to predict the nuclei size distribution for the drop-controlled regime. However, the PD model does not predict the formation of large nuclei or multimodal distributions which were observed in experiments outside the drop-controlled regime. Liu et al. (2013) extended the PD model by including nuclei breakage (Liu et al., 2009), which can have a significant effect on the nuclei size distribution of weak nuclei. In this approach, nuclei breakage is predicted based on the Stokes deformation number (Tardos et al., 1997) but it is still limited to a low dimensionless spray flux. No good quality model to predict the nuclei size distribution for a dimensionless spray flux between 0.1 and 5 is currently available.

In this paper, two new nuclei size distribution models are proposed and assessed. The emphasis of this study is to address the weaknesses of the previously published modelling approaches. For the development of the models, two different approaches are considered, one empirical and one semi-mechanistic. The empirical approach applies the log-normal distribution (LND) function, and the semi-mechanistic approach is based on the PD function. Both models can be included in a PBM framework without increasing the computational cost significantly. MCS data is used to estimate modelling parameters of both models. The model assessment includes comparison to experimental data from the literature. A sensitivity analysis is conducted to assess the MCS modelling assumptions and the applicability of the LND model.

2. Model development

2.1. Log-normal distribution model

An empirical model is proposed that can determine the nuclei size distribution. First, we define the a dimensionless mass frequency and dimensionless nuclei diameter. The dimensionless mass frequency f'_m can be derived from the mass frequency f_m and the diameter of a nucleus formed by a single drop d_1:

$$f'_m = f_m d_1, \tag{4}$$

and the dimensionless nuclei diameter d'_n is defined as the ratio of the nuclei diameter d_n to the diameter of a nucleus formed by a single drop d_1:

$$d'_n = \frac{d_n}{d_1}. \tag{5}$$

The model assumes that the dimensionless nuclei mass frequency follows a log-normal distribution (LND):

$$f'_m(d'_n, \mu_n, \sigma_n) = \frac{1}{d'_n \sigma_n \sqrt{2\pi}} \exp\left(-\frac{(\ln d'_n - \mu_n)^2}{2\sigma_n^2}\right), \tag{6}$$

where μ_n and σ_n are the logarithmic mean and logarithmic standard deviation of the dimensionless nuclei diameter.

It is assumed that the two parameters μ_n and σ_n depend on the dimensionless nucleation number Ψ_n as well as the standard deviation of the spatial drop distribution in the spray σ_x. Based on this assumption, the following two functions are proposed:

$$\mu_n = (m_1\sigma_x + m_2)\Psi_n + m_3 \tag{7}$$

and

$$\sigma_n = (s_1\sigma_x + s_2)\Psi_n + s_3, \tag{8}$$

where m_1, m_2, m_3, s_1, s_2, and s_3 are fitting parameters. Combining Eqs. (6)–(8):

$$f'_m = \frac{1}{d'_n((s_1\sigma_x + s_2)\Psi_n + s_3)\sqrt{2\pi}} \times \exp\left(-\frac{(\ln d'_n - ((m_1\sigma_x + m_2)\Psi_n + m_3))^2}{2((s_1\sigma_x + s_2)\Psi_n + s_3)^2}\right), \tag{9}$$

In order to predict the nuclei size distribution, the diameter of a nucleus formed by a single (average) drop needs to be known. By transformation, the dimensionless results can be converted:

$$f_m = \frac{1}{d_n((s_1\sigma_x + s_2)\Psi_n + s_3)\sqrt{2\pi}} \times \exp\left(-\frac{\left(\ln \frac{d_n}{d_1} - ((m_1\sigma_x + m_2)\Psi_n + m_3)\right)^2}{2((s_1\sigma_x + s_2)\Psi_n + s_3)^2}\right), \tag{10}$$

with

$$d_1 = K_d d_d. \tag{11}$$

The six fitting parameters m_1, m_2, m_3, s_1, s_2, and s_3 need to be estimated; in this study, the average nuclei mass frequency $\bar{f}'_m$

derived from Monte Carlo simulations (MCS) data is used for this purpose. Therefore, a weighted optimisation is chosen with the dimensionless diameter values d'_n as weights, and the final objective function is solved using the least square method:

$$\min_x \sum_{i=1}^{6}\sum_{j=1}^{10}\sum_{k} d'_n(k)\left(\bar{f}'_m(\sigma_x(i),\Psi_n(j),d'_n(k)) - f'_m(\sigma_x(i),\Psi_n(j),d'_n(k),x)\right), \tag{12}$$

with

$$x = [m_1, m_2, m_3, s_1, s_2, s_3]. \tag{13}$$

2.2. Modified Poisson distribution model

The semi-mechanistic Poisson distribution (PD) model approach was proposed by Hapgood et al. (2004, 2009). This approach has been used to predict drop coalescence on powder beds. However, it is also suitable to predict nuclei coalescence by accounting for substituting the smaller drop size with the larger nuclei size. For the development of Hapgood's model, the PD function is applied to determine the probability of a (new) drop/nucleus to coalesce with n other drops/nuclei:

$$P_n = \exp(-\lambda B)\frac{(\lambda B)^n}{n!}, \tag{14}$$

where λ is the intensity of distribution, and B is a subregion. Hapgood et al. (2009) assumed that the intensity λ is a function of the dimensionless spray flux only since drop coalescence was considered. Furthermore, it was assumed that the area that leads to coalescence is 4 times larger than the area of a single drop and is independent of the number of drops already coalesced (See Fig. 2):

$$\lambda B = 4\Psi_a. \tag{15}$$

In this study, nuclei coalescence rather than drop coalescence is assumed. Therefore, the dimensionless nucleation number Ψ_n and the cross-sectional area of a single drop nuclei a_1 are used to determine the intensity of distribution:

$$\lambda = \frac{\Psi_n}{a_1}. \tag{16}$$

In this case, subregion B is the area that leads to nuclei coalescence (nuclei exclusion area). If the centre point of a new drop lands inside this nuclei exclusion area, the drop will coalesce with the nucleus. The nuclei exclusion area is effectively assumed to be one radius larger than the nuclei in every direction. The nuclei exclusion area increases with the number of drops as illustrated in Fig. 2. For the development of the MPD model, the constant nuclei exclusion area is replaced with a function for the nuclei exclusion area a_n which depends on the number of drops:

$$B = a_n(n) \tag{17}$$

From Eqs. (16) and (17), the term λB of the MPD model can be derived:

$$\lambda B = \frac{a_n(n)}{a_1}\Psi_n = k(n)\Psi_n, \tag{18}$$

where $k(n)$ is the ratio of nuclei exclusion area to single nucleus area. Combining Eqs. (14) and (18):

$$P_n = \exp(-k(n)\Psi_n)\frac{(k(n)\Psi_n)^n}{n!}. \tag{19}$$

To represent the spatial distribution of drops, a uniform distribution is assumed in the direction of the powder flow, and a normal distribution is applied perpendicular to the powder flow. Therefore, the spray zone is divided into 10 equal-size sections to model the normal distribution of drops. The nuclei size distribution is determined based on the average dimensionless nucleation number of each section:

$$\Psi_n(x,\mu_x,\sigma_x) = \frac{\bar{\Psi}_n}{P\sigma_x\sqrt{2\pi}}\exp\left(-\frac{(x-\mu_x)^2}{2\sigma_x^2}\right), \tag{20}$$

where x is the coordinate, $\bar{\Psi}_n$ is the dimensionless nucleation number averaged over the spray zone, P is the percentage of drops within the spray zone, and μ_x and σ_x are the mean and the standard deviation of the distribution function, respectively. The following power function is applied to determine the nuclei exclusion area ratio:

$$k(n) = 4 + bn^c, \tag{21}$$

where b and c are fitting parameters. Here, $k(0)$ equals 4 which is the nuclei exclusion area ratio for a single drop nucleus. This power function is the essential contrast to Hapgood's PD model, which assumes: $k(n) = 4$. The average nuclei exclusion area for up to 1000 drops is determined using a MCS approach. A non-linear least squares method is used to fit the following power function to the simulation results.

In order to calculate the factorial of the MPD, Ramanujan's approximation is used (Andrews and Berndt, 2005):

$$n! \approx \sqrt{\pi}\left(\frac{n}{e}\right)^n \sqrt[6]{8n^3 + 4n^2 + n + \frac{1}{88}}. \tag{22}$$

This approximation is also used to scale the equation. Scaling is needed since terms of the PD function can exceed numerical limits of mathematical solvers especially at higher coalescence rates. From Eqs. (19) and (22), the scaled equation can be derived:

$$P_n = \frac{\left(\sqrt[n]{\exp(-k(n)\Psi_n)}\frac{e}{n}k(n)\Psi_n\right)^n}{\sqrt{\pi}\sqrt[6]{8n^3 + 4n^2 + n + \frac{1}{88}}}. \tag{23}$$

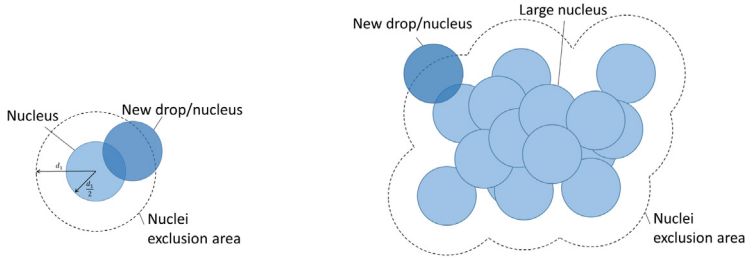

(a) Single drop nucleus (Hapgood's PD model) (b) Large nucleus (MPD model)

Fig. 2. Illustration of nuclei exclusion area and criterion for nuclei coalescence (d_1 single drop nucleus diameter).

While the PD function is normalised, the modifications made lead to a model, which results in a sum of probability greater than 1. The reason for that is the intensity function λB which increases with the number of drops n; the PD function was developed for a constant intensity function. As a consequence, the probability distribution results from Eq. (23) need to be normalised.

After determining the probability distribution using Eq. (23), the nuclei size distribution is determined by discretising the normalised results applying a linear grid with the bin boundaries $d'_{n,k}$:

$$d'_{n,k} = 0.5k. \tag{24}$$

2.3. Monte Carlo simulations for parameter estimation

Two sets of Monte Carlo simulations (MCS) are conducted to determine the model parameters for both models. In the first set of MCS, the entire spray zone is simulated to generate data to fit the empirical LND model (Eq. (10)). The second set of MCS determines the nuclei exclusion area, which is needed for the MPD model (Eq. (21)). In both approaches, the spray zone is assumed to be a flat surface, and nuclei are represented as circles. A flowchart of the simulations is shown in Fig. 3.

In the first set of MCS, circular nuclei are randomly placed on a quadratic area which represents the liquid addition onto a powder bed surface using a nozzle. This approach is adapted from Wildeboer et al. (2005). The simulations are based on only one input parameter - the dimensionless nucleation number. The circles represent nuclei because the approach is based on nuclei coalescence rather than drop coalescence. Instead of representing the spray as drops which vary in size (Wildeboer et al., 2005), a uniform drop diameter is assumed in this case. In the direction of the powder flow, the spatial distribution of drops is assumed to be uniform over the spray zone because surface of the powder bed is moving steadily through the spray zone. A truncated normal distribution is applied perpendicular to the direction of the powder flow:

$$N(x, \mu_x, \sigma_x) = \frac{1}{P\sigma_x\sqrt{2\pi}} \exp\left(-\frac{(x-\mu_x)^2}{2\sigma_x^2}\right), \tag{25}$$

where x is the coordinate, P is the percentage of drops within the spray zone, and μ_x and σ_x are the mean and the standard deviation of the distribution function, respectively. The mean location is set to the centre of the spray zone, and the standard deviation is varied between 0.15 and 0.25 of the width of the spray zone, which is a typical range for spray systems (Wauters et al., 2002; Sehmbi, 2019). In order to determine whether or not nuclei coalesce, an overlapping criterion is applied:

$$(x_i - x_j)^2 + (y_i - y_j)^2 \leqslant \frac{(d_{1,i} + d_{1,j})^2}{4}, \tag{26}$$

where x and y are the centre coordinates of the drops i and j. Based on this criterion, nuclei are identified, and their sizes are determined. The results are discretised to generate a nuclei size distribution using a linear grid. The bin boundaries $d'_{n,k}$ are given by:

$$d'_{n,k} = 0.5k. \tag{27}$$

The size of the spray zone is 2000 × 2000 pixels, and the single drop nuclei diameter d_1 is 10 pixels. The number of drops per simulation varies between 5100 and 51000 which correlates to a dimensionless nucleation number between 0.1 and 1.0. The MCS results are averaged over 10 simulations. Python is used to carry out all MCS; one simulation can take between several minutes and several hours depending on the dimensionless nucleation number used.

Additional MCS are carried out based on the same approach. In these simulations, the following inputs are varied: the standard deviation of the spatial drop distribution in the direction perpendicular to the powder flow ($\frac{1}{16} - \frac{1}{2}$ of the spray zone width) and the nuclei diameter (10–20 pixels). Furthermore, a log-normal drop size distribution is introduced with a logarithmic standard deviation between 0.1 and 0.6 of the logarithmic mean diameter.

In the second set of MCS, nuclei with up to a 1000 drops are simulated. The objective is to determine the average nuclei exclusion area (Fig. 2). Therefore, every drop is added individually; and after every drop, the nuclei exclusion area is determined. Every drop (except for the first drop) is placed randomly applying a uniform distribution with a minor constraint: the new drop has to overlap with the existing nucleus (Overlapping criterion: Eq. (26)). The final results are averaged over 100 simulations.

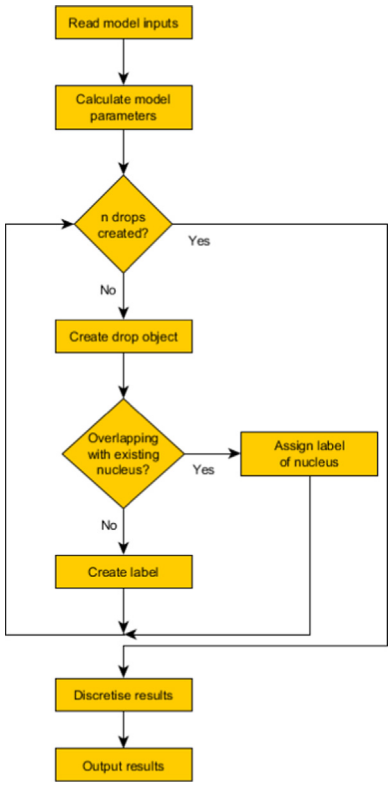

Fig. 3. Flowchart of the MCS (Wildeboer et al., 2005).

2.4. Model assessment

For the model validation and assessment, the deviation of the model results from the reference data at every grid point is determined, and the sum of squared errors is calculated. To be able to utilise different sets of reference data, the relative sum of squared errors is reported, while all results are relative to the results of Hapgood's PD model.

3. Literature experiments for model validation

In order to assess the model predictions, experimental data is used, as well as MCS data. The deviation of the model predictions is quantified with the sum of squared errors at every grid point. The results reported are relative to Hapgood's PD model results.

Two sets of experiments are selected which were published by Litster et al. (2001, 2002). An overview of all experiments can be found in Table 1.

Table 1
Overview of experiments.

Source	Equipment	Dimensionless nucleation number Ψ_n [−]
Litster et al. (2001)	Ex-granulator	0.5; 0.6; 0.7; 1.2; 2.7
Litster et al. (2002)	High-shear mixer	0.5; 0.7; 1.2

Litster et al. (2001) conducted ex-granulator nucleation experiments using a powder bed on a rotating table with different rotational velocities. A nozzle was placed above the powder bed to spray liquid onto the powder bed. Litster et al. (2002) conducted nucleation-only experiments in a Fielder PharmaMATRIX 25 l high-shear mixer with a spraying time of 5 s. Experiments at different impeller frequencies are conducted to test the impact of the dimensionless nucleation number on the nuclei size distribution.

In all experiments, the powder bed consisted of lactose monohydrate which was screened before to facilitate the separation of nuclei during the characterisation. Water was used as binder liquid which was delivered by a single flat spray nozzle. The spray pressure applied was 3.1 bar, which lead to an average drop diameter of 96 m, a spray rate of 58 $\frac{\text{ml}}{\text{min}}$, and a spray zone width of 8 cm. A standard deviation of the spatial drop distribution of 0.25 can be derived from characterisation measurements for the spray nozzle and pressure applied (Wauters et al., 2002), and a nuclei-to-drop diameter ratio of 1.5 has been determined. The experiments are described in more detail by Litster et al. (2001, 2002), Hapgood et al. (2004, 2009).

4. Results and discussion

The nuclei size distribution in the spray zone is simulated using MCS, and a selection of the results are illustrated in Fig. 4. The MCS results show clearly the uniform distribution in the vertical direction and the normal distribution horizontally.

4.1. Log-normal distribution model

First, two parameter estimation studies are carried out to estimate parameter values for the log-normal distribution (LND) model (Eq. (9)). Therefore, the model is fitted to the MCS results for each dimensionless nucleation number individually (1 st parameter estimation; Eq. (6)) and for all conditions simultaneously (2 nd parameter estimation; Eq. (9)). A comparison of the parameter values of both studies is shown in Fig. 5. The results of the 1 st parameter estimation show that the values estimated increase almost linearly with increasing dimensionless nucleation number. Furthermore, it can be seen that both parameter estimation studies result in very similar parameters for the dimensionless nucleation number range chosen. This confirms that both model parameters can be represented with linear functions of the dimensionless nucleation number only (Eqs. (7) and (8)). The results of the parameter estimation are given including a 95% confidence interval (using Eq. (9)):

$$m_1 = -3.0 \pm 0.88 \tag{28}$$
$$m_2 = 1.9 \pm 0.18 \tag{29}$$
$$m_3 = -0.046 \pm 0.050 \tag{30}$$
$$s_1 = -3.4 \pm 0.87 \tag{31}$$
$$s_2 = 0.98 \pm 0.18 \tag{32}$$
$$s_3 = 0.32 \pm 0.024. \tag{33}$$

The Monte Carlo simulations (MCS) and the fitted LND model results are compared in Fig. 6. The MCS data shows that most nuclei do not coalesce at a low dimensionless nucleation number, giving a very narrow size distribution. With increasing dimensionless nucleation number, more larger nuclei are predicted. Due to the formation of more larger nuclei, a distribution with a long tail is predicted. However, the peak of the mass frequency remains at a very small nuclei diameter. The fitted LND model results agree very well with the MCS at low as well as high dimensionless nucleation number values. The narrow size distribution at a low dimension-

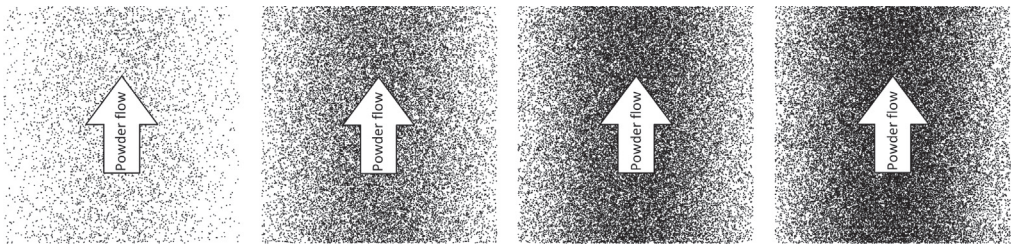

(a) $\Psi_n = 0.1$ (b) $\Psi_n = 0.5$ (c) $\Psi_n = 0.8$ (d) $\Psi_n = 1.0$

Fig. 4. Surface area coverage in spray zone at different dimensionless nucleation number values from MCS data ($\sigma_x = 0.25$).

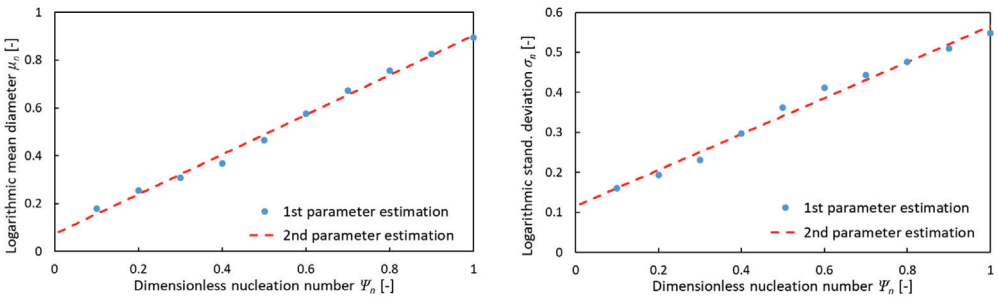

(a) Logarithmic mean diameter (b) Logarithmic standard deviation of the diameter

Fig. 5. Parameter values estimated in the 1st and 2nd parameter estimation using Eqs. (6) and (9), respectively, of the LND model ($\sigma_x = 0.25$).

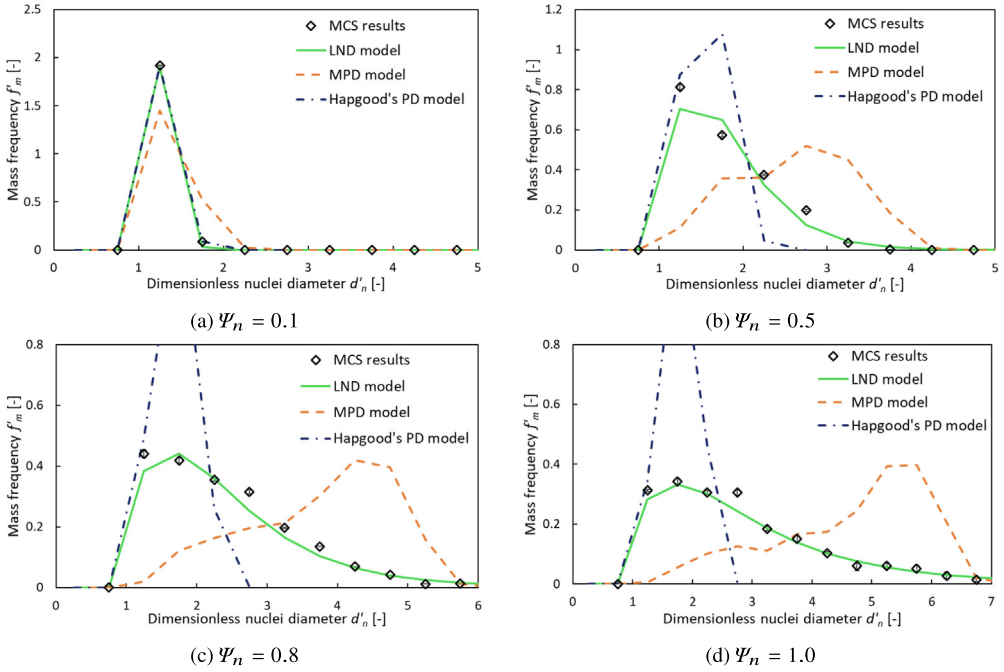

Fig. 6. Comparison of the LND, MPD, and Hapgood's PD model results with MCS data ($\sigma_x = 0.25$).

less nucleation number is correctly represented as well as the long tail at a higher dimensionless nucleation number. This shows that the LND model is suitable for representing the MCS data for the dimensionless nucleation number range chosen. The LND model can be applied to predict the nuclei size distribution for a wide range of conditions using the parameter values reported (Eqs. (28)–(33)).

4.2. Poisson distribution model

The nuclei exclusion area results determined using MCS can be found in Fig. 7. The 95% confidence interval of the MCS shows that the uncertainty of the results is an acceptable range. Furthermore, it can be seen that the power function fitted is in very good agreement with the simulation results. The parameters b and c of Eq. (21) are estimated, and the respective 95% confidence intervals are determined:

$$b = 2.70 \pm 0.01 \tag{34}$$

$$c = 0.708 \pm 0.001 \tag{35}$$

In Fig. 6, the MPD model and Hapgood's PD model are compared to MCS data. The MCS data used for this comparison is not used to estimate model parameters of the MPD model, and Hapgood's PD model does not require any parameter estimation. Therefore, all model results compared to MCS data in this section are predictions. Hapgood's PD model predicts the nuclei size distribution for $\Psi_n = 0.1$ very accurately. Also, the mass frequency of small nuclei ($d'_n < 1.5$) is in very good agreement with the MCS data which corresponds with previous model assessment results (Hapgood et al., 2004). As described in Section 2.2, only the area of larger nuclei is underpredicted but the area of very small nuclei is determined accurately. The fact that this model is capable of predicting specific MCS results shows the strength of this model; the MCS approach is very computationally expensive compared to Hapgood's PD model. However, the nuclei size distribution is clearly underpredicted outside the drop-nucleation regime because the formation of larger nuclei is not predicted (Fig. 6b,c,d).

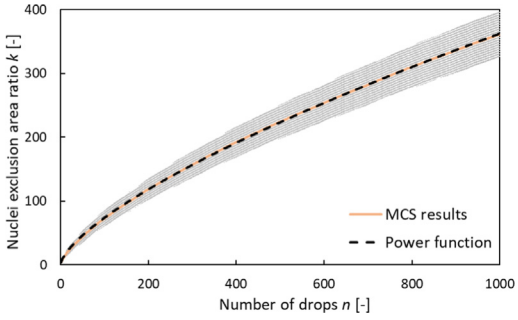

Fig. 7. Average exclusion area ratio with a 95% confidence interval from MCS data and the power function fitted.

While the predictions of the MPD model agree reasonably well at lower dimensionless nucleation numbers, the discrepancy of the predictions becomes apparent at higher dimensionless nucleation numbers. Both the MCS and the MPD model predict the average nuclei size to increase; however, the resulting distributions do not match. The MCS results show a much broader distribution at higher dimensionless nucleation numbers with a long tail of large nuclei while the peak of the distribution remains always at $d'_n \approx 1-2$. This is in contrast to the MPD model predictions which show a narrower nuclei size distribution and a large increase of the peak at higher dimensionless nucleation numbers. The MPD model does not contain an overlapping criterion like the MCS. It solely determines the likelihood of n nuclei/drops to land within the area $a_n(n)$ (average nuclei exclusion area formed by n drops). This can lead to an overprediction of larger nuclei since the drops that land in a_n do not necessarily overlap.

A quantitative comparison of the accuracy of the model predictions can be found in Fig. 9. Hapgood's PD model underpredicts the nuclei size distribution outside the drop-controlled regime while the MPD model overpredicts the nuclei size distribution. Neither model captures the breadth of the nuclei size distributions at $\Psi_n \geqslant 0.5$.

4.3. Comparison of model predictions with experimental results

Both the semi-mechanistic MPD model and the empirical LND model are compared to experimental data from Litster et al. (2001, 2002) in order to assess the accuracy of the model results. Although these two models require parameter fitting, only MCS results are used for this purpose. The experimental data shown is only used to assess model predictions. The experiments selected are ex-granulator experiments as well as nucleation-only experiments in a high-shear mixer. The dimensionless nucleation number in these experiments ranges between 0.5 and 2.7.

The model predictions are compared to the experimental data in Fig. 8. The experimental data shows a narrow distribution with a small average size at lower dimensionless nucleation numbers, which indicates that only few drops coalesced to agglomerates. However, a significantly broader bi-modal distribution is obtained at higher dimensionless nucleation numbers ($\Psi_n = 1.2, 2.7$), which confirms the speculation that drop coalescence on the powder bed surface can have a significant effect on the nuclei size distribution. Nevertheless, the (first) peak of the distribution remains at a low nuclei diameter, even at the highest nucleation number tested ($\Psi_n = 2.7$). A comparison between the two experimental techniques shows that the high-shear mixer experiments (Fig. 8b,e,g) result in a slightly larger nuclei size distribution than the ex-granulator experiments (Fig. 8a,d,f) even at the same dimensionless nucleation number Ψ_n. This potentially indicates nuclei growth during the high-shear mixer experiments, which is not considered by any of the models assessed.

The MPD model predictions diverge from the experimental results. At lower dimensionless nucleation numbers, the

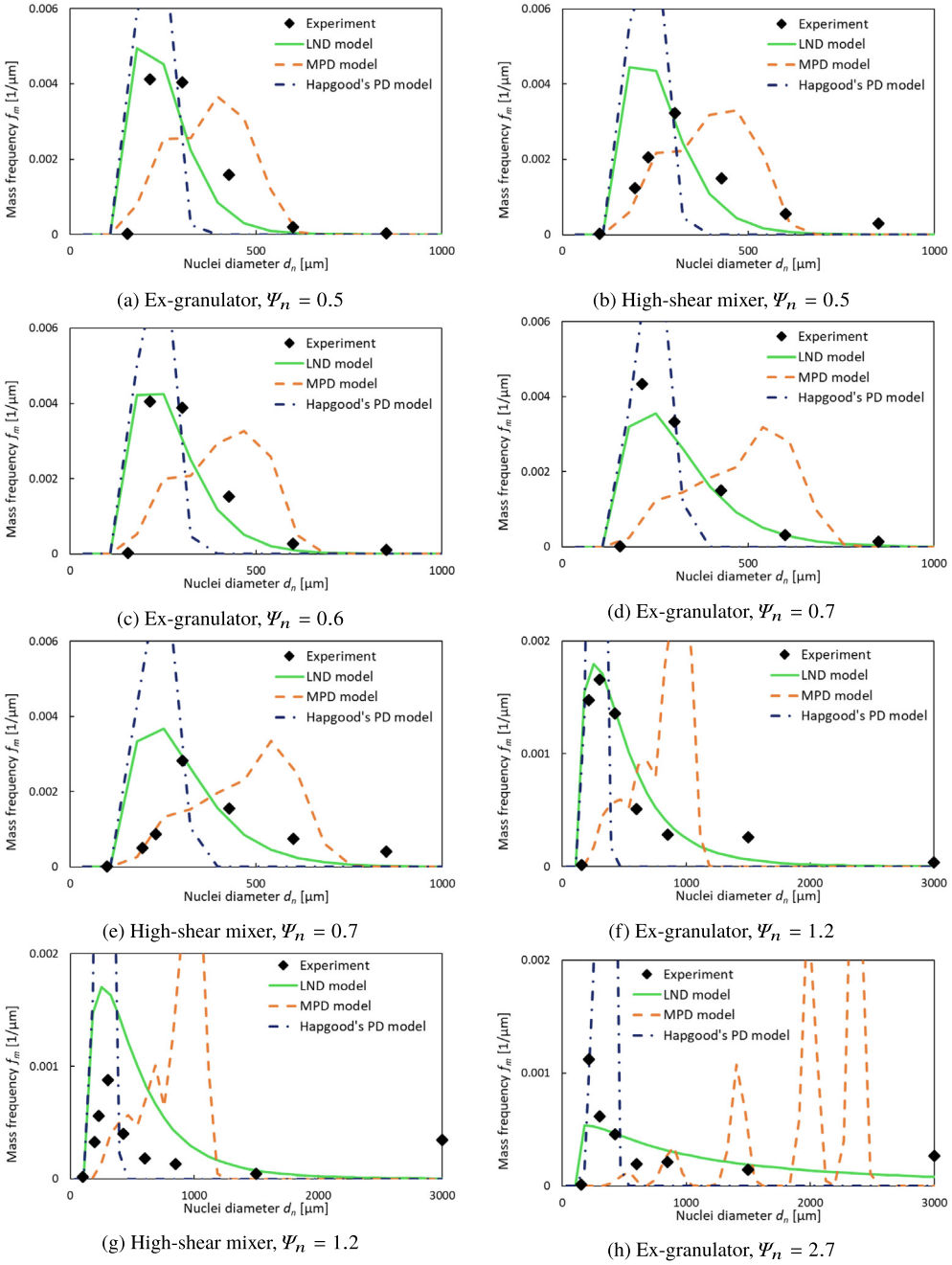

Fig. 8. Comparison of model results with experimental data (Ψ_n dimensionless nucleation number).

experimental nuclei size distributions are slightly overpredicted; and with increasing dimensionless nucleation number, the MPD model predicts a shift of the peak to larger nuclei diameters rather than a significantly broader distribution. The LND model results are in good agreement with the experimental data at lower dimensionless nucleation numbers, which are within the empirical design space of this model ($\Psi_n \leqslant 1.0$). A comparison with experimental data outside the empirical design space shows a qualitative mismatch because bi-modal distributions are not predicted. Nevertheless, broad distributions are predicted which capture the experimental data reasonably well.

The performance is also assessed quantitatively based on the sum of squared errors. The results show that the LND model provides the most accurate predictions out of all the models evaluated (Fig. 9). Overall, the LND model agrees well with the experimental data, even though the experimental conditions were not fully characterised and reported. Therefore, the LND model can be applied to a wide range of wet granulation processes that operate under similar conditions. The fact that the LND model does not only agree with ex-granulator results but also with nucleation-only experiments in a high-shear mixer shows that this model can be applied to predict the nuclei size distribution in different wet granulation processes.

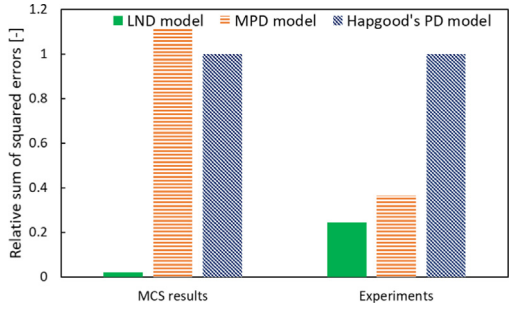

Fig. 9. Sum of squared errors of the model results to MCS and experimental data (relative to Hapgood's PD model results).

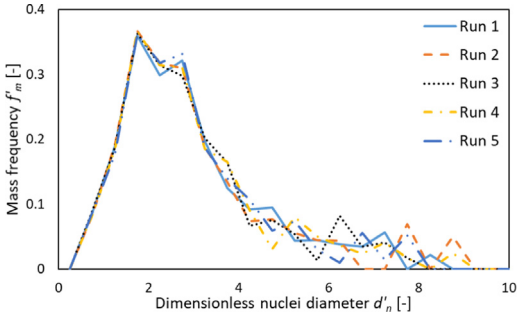

Fig. 10. Assessment of repeatability based on 5 MCS with default settings.

4.4. Sensitivity analysis for the LND model

A sensitivity analysis is conducted to gain more insight into the LND model results. The sensitivity analysis is based on Monte Carlo simulations (MCS) data which have been used to estimate the parameter values for the LND model. These MCS are based on assumptions about the spray characteristics which should capture experimental conditions well. In this sensitivity analysis, the effects of the spray characteristics on the results are studied, and the critical assumptions, which have to be validated experimentally, are identified. All MCS results shown are obtained applying the default settings with $\Psi_n = 1.0$ as described in Section 2.3 unless reported otherwise.

First, the repeatability of MCS is assessed. For this purpose, the results from 5 simulations are compared in Fig. 10. A slight quantitative difference between the results can be noticed at large nuclei diameter. However, the uncertainty is rather low and the resulting distributions are qualitatively equivalent. Consequently, a qualitative assessment can be based on a sensitivity analysis without averaging MCS results.

A normal spatial drop distribution with a standard deviation σ_x of $\frac{1}{4}$ is applied in the MCS. In order to understand the impact of the spatial drop distribution on the nuclei size distribution, the standard deviation of the normal distribution is varied as shown in Fig. 11. The results show that although the location of the (first) peak of the nuclei size distribution remains unchanged, a much broader or narrower nuclei size distribution can be observed when the spatial distribution varied. While a broader spatial distribution ($\sigma_x = \frac{1}{2}$) results in a very narrow nuclei size distribution with no large nuclei, a very narrow spatial distribution ($\sigma_x = \frac{1}{8}; \frac{1}{16}$) generates a very broad spatial distribution with few very large nuclei. With $\sigma_x = \frac{1}{2}$, the distribution is almost uniform and the dimensionless nucleation number is similar across the whole spray zone. At $\sigma_x = \frac{1}{16}$, the dimensionless nucleation number is very high at the centre and very low at the edges, leading to a very broad nuclei size distribution. This shows that the spatial drop distribution has a significant impact and should therefore be well characterised for the nozzle system of interest.

The uniform drop size assumption is assessed by introducing a log-normal drop size distribution while maintaining a constant Sauter mean diameter (Fig. 12). As the results show, the spray drop size distribution has a very small impact on the nuclei size distribution, which is of the same of magnitude as the uncertainty (See Fig. 10). Overall, it can be concluded that a mono-modal drop

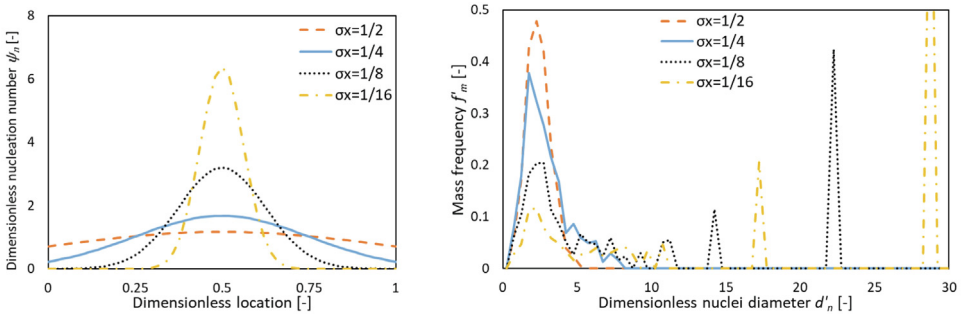

(a) Spatial drop distribution (b) Nuclei size distribution

Fig. 11. Assessment of the impact of the spatial drop distribution on the nuclei size distribution (σ_x standard deviation of the normal distribution).

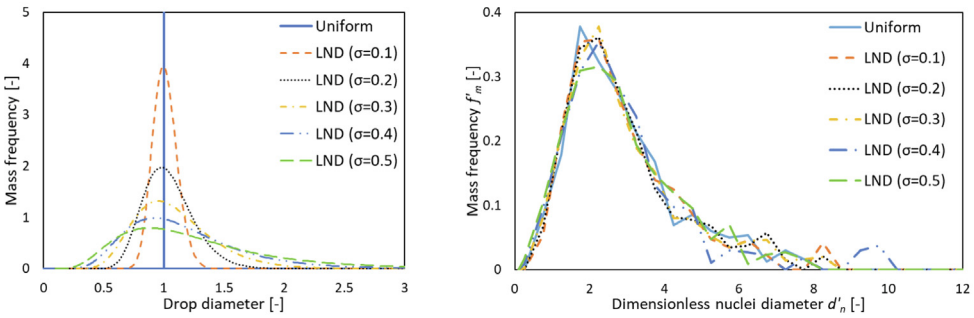

(a) Spray drop size distribution (b) Nuclei size distribution

Fig. 12. Assessment of the impact of the spray drop size distribution on the nuclei size distribution with a constant Sauter mean diameter (σ logarithmic standard deviation of drop size distribution).

size distribution can be assumed to be uniform for this purpose. However, only log-normal drop size distributions with a maximum logarithmic standard deviation σ of 0.5 have been tested in this sensitivity analysis. Even broader or multi-modal drop size distributions could have a significant impact on the nuclei size distribution.

The effect of increasing the mean drop diameter while keeping the volumetric flowrate constant is also tested (Fig. 13). According to Eq. (3), the dimensionless nucleation number decreases as a result. As expected, the results show that an increase in drop diameter results in an increase of minimum nuclei size. However, due to the constant volumetric flowrate, the total cross-sectional area of drops (and consequently the dimensionless nucleation number) decreases which leads to less coalescence. The resulting nuclei size distribution is significantly narrower with less large lumps due to the drop diameter increase. This results show that measuring the mean drop diameter is essential to predict the breadth of the nuclei size distribution.

The LND model with the parameter values reported (See Section 4.1) can be applied to any process if the MCS assumptions capture the spray characteristics well. In practice, deviations of the spatial drop distribution and the spray drop size distribution are expected. Considerable deviations from the MCS assumptions might require additional MCS data to re-estimate the parameters before the LND model can be applied.

4.5. Recommendations for nuclei models to use in PBM

Based on the results presented in this paper, we recommend the LND model (Eqs. (7)–(9)) for systems with any spray flux from 0 to 5. The model parameters m_1, m_2, m_3, s_1, s_2, and s_3 are sensitive to spatial drop distribution and will need to be recalibrated with MCS from the values given in Eqs. (28)–(33) if the standard deviation of this distribution is distinctively outside the range used in this study (0.15 to 0.25). That aside, this is a simple, general and very robust model for incorporation in process level population balance models for high shear, tumbling and fluidised granulators that meet the criteria for immersion nucleation. The spray characteristics required as input for the model (spray geometry, spray drop size, and spatial drop distribution) are relatively easy to measure using standard techniques.

There is an implicit assumption in this model that drop immersion into the powder bed is fast ($\tau_p < 0.1$) and it can be assumed that the nuclei form instantaneously. This is common in practice where a low viscosity binder is used that wets the powder bed well. Where the binder liquid is more viscous or the powder is very fine, we may have a case where $\tau_p > 0.1$. The kinetics of the immersion process cannot be neglected, and powder will take a finite time to imbibe into the drop. This process can be modelled using the model of Hounslow et al. (2009) where the LND model can still be used to describe the drop size distribution that is the starting point for the immersion process.

In some specialist applications such as detergent manufacture, where extremely viscous or semi solid binders are used, binders cannot be atomised in a nozzle. For these cases, the LND model is not applicable. Instead, a breakage model for nuclei formation in needed to determine the initial binder "drop" distribution (Davis, 2016), and Hounslow's immersion model can still be used to account for the kinetics by which solid is embedded into the binder particle. Thus, we now have a suite of models that can be used to cover the full range of behaviours on Hapgood's regime map (see Fig. 14).

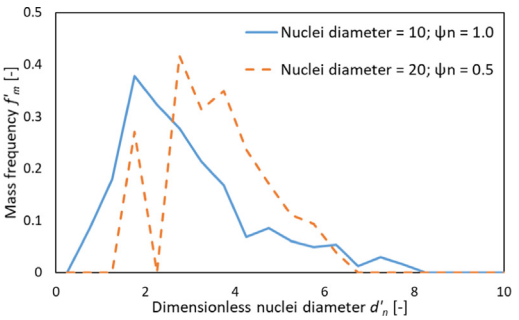

Fig. 13. Assessment of mean drop size with a constant volumetric flowrate (Ψ_n dimensionless nucleation number).

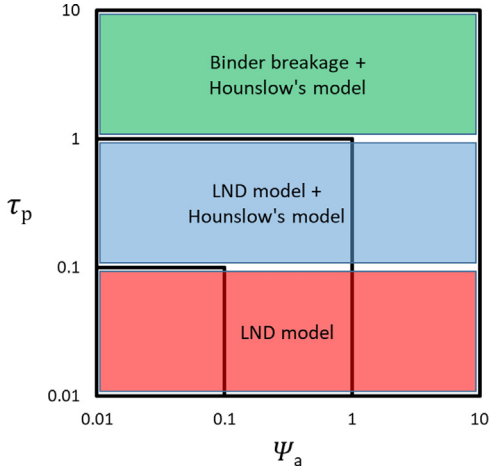

Fig. 14. Choice of model for granule nucleation for the full nucleation regime map.

5. Conclusions

The LND model is able to represent MCS data very accurately at low and high dimensionless nucleation numbers. The model results are also in good agreement with experimental results, even at dimensionless nucleation numbers well above 1. While the MPD model gives acceptable predictions at low dimensionless nucleation numbers, it fails to predict MCS and experimental data at high dimensionless nucleation numbers. Both models are a significant improvement of the state of the art (Hapgood's PD model (Hapgood et al., 2009)), which underpredicts the nuclei size distribution significantly outside the drop-nucleation regime.

The LND model is suitable for determining the nuclei size distribution and can be easily applied for process modelling studies. A sensitivity analysis has shown that the spray characteristics have a major impact on the nuclei size distribution. Especially, the spatial drop distribution in the spray needs to determined because the LND model requires it as an input parameter, and the MCS assumption about the drop size distribution needs to be validated experimentally before applying the LND model. A PD model could reduce the high computational effort that is required for MCS. Moreover, selected results are in very good agreement with MCS data. Nevertheless, a coalescence criterion that captures this mechanism well is required before the PD function can be applied for this purpose.

Declaration of Competing Interest

The authors declare that they have no known competing financial interests or personal relationships that could have appeared to influence the work reported in this paper.

Acknowledgements

The authors would like to acknowledge F. Hoffmann-La Roche AG for sponsoring this work, and for allowing us to use their laboratory facilities and equipment.

References

Andrews, G.E., Berndt, B.C., 2005. Ramanujan's Lost Notebook, vol. 1. Springer, Berlin, New York.
Ax, K., Feise, H., Sochon, R., Hounslow, M., Salman, A., 2008. Influence of liquid binder dispersion on agglomeration in an intensive mixer. Powder Technol. 179, 190–194.
Barrasso, D., El Hagrasy, A., Litster, J.D., Ramachandran, R., 2015. Multi-dimensional population balance model development and validation for a twin screw granulation process. Powder Technol. 270, 612–621.
Barrasso, D., Ramachandran, R., 2016. Qualitative assessment of a multi-scale, compartmental PBM–DEM model of a continuous twin-screw wet granulation process. J. Pharmaceut. Innovat. 11, 231–249.
Biggs, C.A., Sanders, C., Scott, A.C., Willemse, A.W., Hoffman, A.C., Instone, T., Salman, A.D., Hounslow, M.J., 2003. Coupling granule properties and granulation rates in high-shear granulation. Powder Technol. 130, 162–168.
Bouffard, J., Bertrand, F., Chaouki, J., 2012. A multiscale model for the simulation of granulation in rotor-based equipment. Chem. Eng. Sci. 81, 106–117.
Chaudhury, A., Barrasso, D., Pandey, P., Wu, H., Ramachandran, R., 2014. Population balance model development, validation, and prediction of CQAs of a high-shear wet granulation process: towards QbD in drug product pharmaceutical manufacturing. J. Pharmaceut. Innovat. 9, 53–64.
Chaudhury, A., Barrasso, D., Pohlman, D.A., Litster, J.D., Ramachandran, R., 2017. Mechanistic modeling of high-shear and twin screw mixer granulation processes. In: Pandey, P., Bharadwaj, R. (Eds.), Predictive Modeling of Pharmaceutical Unit Operations. Woodhead Publishing, pp. 99–135.
Darelius, A., Brage, H., Rasmuson, A., Björn, I.N., Folestad, S., 2006. A volume-based multi-dimensional population balance approach for modelling high shear granulation. Chem. Eng. Sci. 61, 2482–2493.
Davis, N.J., 2016. Mechanical dispersion of semi-solid binders in high-shear granulation Ph.D. thesis. Purdue University.
Dhanarajan, A.P., Bandyopadhyay, R., 2007. An energy-based population-balance approach to model granule growth and breakage in high-shear wet granulation processes. AAPS PharmSciTech 8, E118–E125.
Hapgood, K.P., Litster, J.D., Biggs, S.R., Howes, T., 2002. Drop penetration into porous powder beds. J. Colloid Interface Sci. 253, 353–366.
Hapgood, K.P., Litster, J.D., Smith, R., 2003. Nucleation regime map for liquid bound granules. AIChE J. 49, 350–361.
Hapgood, K.P., Litster, J.D., White, E.T., Mort, P.R., Jones, D.G., 2004. Dimensionless spray flux in wet granulation: Monte-Carlo simulations and experimental validation. Powder Technol. 141, 20–30.
Hapgood, K.P., Tan, M.X., Chow, D.W., 2009. A method to predict nuclei size distributions for use in models of wet granulation. Adv. Powder Technol. 20, 293–297.
Hounslow, M.J., Oullion, M., Reynolds, G.K., 2009. Kinetic models for granule nucleation by the immersion mechanism. Powder Technol. 189, 177–189.
Kariuki, W.I., Freireich, B., Smith, R.M., Rhodes, M., Hapgood, K.P., 2013. Distribution nucleation: quantifying liquid distribution on the particle surface using the dimensionless particle coating number. Chem. Eng. Sci. 92, 134–145.
Kastner, C.A., Brownbridge, G.P.E., Mosbach, S., Kraft, M., 2013. Impact of powder characteristics on a particle granulation model. Chem. Eng. Sci. 97, 282–295.
Kumar, A., Gernaey, K.V., De Beer, T., Nopens, I., 2013. Model-based analysis of high shear wet granulation from batch to continuous processes in pharmaceutical production–a critical review. Eur. J. Pharm. Biopharm. 85, 814–832.
Kumar, A., Vercruysse, J., Mortier, S.T.F.C., Vervaet, C., Remon, J.P., Gernaey, K.V., De Beer, T., Nopens, I., 2016. Model-based analysis of a twin-screw wet granulation system for continuous solid dosage manufacturing. Comput. Chem. Eng. 89, 62–70.
Le, P.K., Avontuur, P., Hounslow, M.J., Salman, A.D., 2009. The kinetics of the granulation process: right from the early stages. Powder Technol. 189, 149–157.
Lee, K.F., Dosta, M., McGuire, A.D., Mosbach, S., Wagner, W., Heinrich, S., Kraft, M., 2017. Development of a multi-compartment population balance model for high-shear wet granulation with discrete element method. Comput. Chem. Eng. 99, 171–184.
Litster, J.D., Hapgood, K.P., Michaels, J.N., Sims, A., Roberts, M., Kameneni, S.K., 2002. Scale-up of mixer granulators for effective liquid distribution. Powder Technol. 124, 272–280.
Litster, J.D., Hapgood, K.P., Michaels, J.N., Sims, A., Roberts, M., Kameneni, S.K., Hsu, T., 2001. Liquid distribution in wet granulation: dimensionless spray flux. Powder Technol. 114, 32–39.
Liu, L.X., Smith, R., Litster, J.D., 2009. Wet granule breakage in a breakage only high-hear mixer: Effect of formulation properties on breakage behaviour. Powder Technol. 189, 158–164.
Liu, L.X., Zhou, L., Robinson, D.J., Addai-Mensah, J., 2013. A nuclei size distribution model including nuclei breakage. Chem. Eng. Sci. 86, 19–24.
Oullion, M., Reynolds, G.K., Hounslow, M.J., 2009. Simulating the early stage of high-shear granulation using a two-dimensional Monte-Carlo approach. Chem. Eng. Sci. 64, 673–685.
Pitt, K., Smith, R.M., de Koster, S.A.L., Litster, J.D., Hounslow, M.J., 2018. Kinetics of immersion nucleation driven by surface tension. Powder Technol. 335, 62–69.
Pohlman, D.A., Litster, J.D., 2015. Coalescence model for induction growth behavior in high shear granulation. Powder Technol. 270, 435–444.
Poon, J.M.-H., Immanuel, C.D., Doyle III, F.J., Litster, J.D., 2008. A three-dimensional population balance model of granulation with a mechanistic representation of the nucleation and aggregation phenomena. Chem. Eng. Sci. 63, 1315–1329.
Poon, J.M.-H., Ramachandran, R., Sanders, C.F.W., Glaser, T., Immanuel, C.D., Doyle III, F.J., Litster, J.D., Stepanek, F., Wang, F.-Y., Cameron, I.T., 2009. Experimental validation studies on a multi-dimensional and multi-scale population balance model of batch granulation. Chem. Eng. Sci. 64, 775–786.
Ramachandran, R., Immanuel, C.D., Stepanek, F., Litster, J.D., Doyle III, F.J., 2009. A mechanistic model for breakage in population balances of granulation: Theoretical kernel development and experimental validation. Chem. Eng. Res. Des. 87, 598–614.
Ramkrishna, D., Mahoney, A.W., 2002. Population balance modeling. promise for the future. Chem. Eng. Sci. 57, 595–606.
Sanders, C.F.W., Willemse, A.W., Salman, A.D., Hounslow, M.J., 2003. Development of a predictive high-shear granulation model. Powder Technol. 138, 18–24.
Sehmbi, H., 2019. Investigation of nucleation in high shear wet granulation Master's thesis. The University of Sheffield.
Tardos, G.I., Khan, M.I., Mort, P.R., 1997. Critical parameters and limiting conditions in binder granulation of fine powders. Powder Technol. 94, 245–258.
Verkoeijen, D., Pouw, G.A., Meesters, G.M.H., Scarlett, B., 2002. Population balances for particulate processes-a volume approach. Chem. Eng. Sci. 57, 2287–2303.
Wauters, P.A.L., Jakobsen, R.B., Litster, J.D., Meesters, G.M.H., Scarlett, B., 2002. Liquid distribution as a means to describing the granule growth mechanism. Powder Technol. 123, 166–177.
Wauters, P.A.L., Scarlett, B., Liu, L.X., Litster, J.D., Meesters, G.M.H., 2003. A population balance model for high shear granulation. Chem. Eng. Commun. 190, 1309–1334.
Wildeboer, W.J., Koppendraaier, E., Litster, J.D., Howes, T., Meesters, G., 2007. A novel nucleation apparatus for regime separated granulation. Powder Technol. 171, 96–105.
Wildeboer, W.J., Litster, J.D., Cameron, I.T., 2005. Modelling nucleation in wet granulation. Chem. Eng. Sci. 60, 3751–3761.
Yu, X., Hounslow, M.J., Reynolds, G.K., 2016. Representing spray zone with cross flow as a well-mixed compartment in a high shear granulator. Powder Technol. 297, 429–437.
Yu, X., Hounslow, M.J., Reynolds, G.K., Rasmuson, A., Niklasson Björn, I., Abrahamsson, P.J., 2017. A compartmental CFD–PBM model of high shear wet granulation. AIChE J. 63, 438–458.
Žižek, K., Hraste, M., Gomzi, Z., 2013. High shear granulation of dolomite–I: Effect of shear regime on process kinetics. Chem. Eng. Res. Des. 91, 70–86.